*Wasit Journal of Engineering Sciences*
Journal homepage: https://ejuow.uowasit.edu.iq
Vol. 14 No. 2 June 2026, pp.40-51
https://doi.org/10.31185/ejuow.v14i2.718

ISSN 2305-6932
*Original Research*

# Analysis and Stepwise Regression of Flexural Load-Capacity of Steel Wire-Reinforced Precast Concrete Sandwich Panels

**Khaldoon S. A. Altameemi[1], Omar M. H. Chlaibawi[1], Sallal R. Abid[1], Mustafa Özakça[2]**
[1] Civil Engineering Department, College of Engineering, Wasit University, Iraq
[2] Civil Engineering Department, College of Engineering, Gaziantep University, Turkey

***Corresponding Author Email: Std2023203.K.S@uowasit.edu.iq***

Received June. 3, 2025 | Revised Aug.10, 2025 | Accepted. Oct.22, 2025 | Online Jun.1, 2026

## ABSTRACT

Precast Sandwich Panel (PSP) is a plate element that is lighter, cheaper, and has significantly better thermal insulation compared to conventional concrete plates, which are typically used as wall or slab units. The positive features of PSP make it a probable solution for many construction issues in Iraq related to low-cost energy-saving housing, temporary camping, and industrial units, which call for extensive analysis, experimental, and numerical studies to explore the pros and cons of PSPs as a low-cost roofing solution. The aim of this study is to evaluate the degree of influence of the geometry, material, and design parameters on the flexural capacity of PSPs and to introduce a pre-design evaluation tool using multivariable stepwise regressions. Experimental data, including 13 input parameters related to the properties of the outer concrete layers, inner insulation core, and shear connectors between them, in addition to cracking and ultimate loads as outputs, were analyzed for 50 experimental steel wire-reinforced sandwich plates. Direct correlations showed that none of the studied parameters has a significant sole impact on the flexural strength of the panels, while stepwise regressions showed that most of these parameters are effective. P-values higher than 5% were recorded for some parameters, which were automatically excluded from the regression models, while the T- and F-values revealed different influence degrees for the included parameters. Finally, two multi-variable stepwise regression models were introduced for cracking and ultimate loads with determination coefficients ($R^2$) values of 89.3 and 92.6%, respectively, which reflect their high reliability as pre-design simplified analysis tools.

**Keywords**: Precast sandwich plate; stepwise regression; steel wire-reinforcement; flexural strength; cracking load.

## 1. Introduction

Three major issues, in addition to others, decelerate the growth of the housing construction industry and its efficiency in the Iraqi community. These issues are the relatively high cost of construction materials and works, the extremely hot weather that extends along the summer in addition to significant parts of spring and autumn, and the balance of energy consumption demand and production, which is also related to weather conditions. Precast Sandwich Panels (PSP) are plate members that can be used as walls or roofing elements, which are typically composed of two outer concrete thin membrane elements separated by a thicker layer of an insulation material like expanded polystyrene [1]. The outer reinforced layers are responsible for carrying loads and offering fire protection, while the insulation core is responsible for decelerating thermal conductivity and providing thermal insulation [2].

This system can be considered a fit solution to overcome the three above-mentioned construction issues. Firstly, it can be considered a low-cost technique, where the required steel and concrete materials and finishing costs are significantly lower than in traditional building techniques. Secondly, the PSP system facilitates a quicker construction process, where no in-site forms, reinforcement, concrete casting, and curing waiting periods are

required, in addition to the reduction of their costs from the total construction cost. Thirdly, the thermal insulation offered by the core would significantly keep more stable interior temperatures that would significantly reduce the demand of energy. However, despite the distinguished advantages of PSPs, one of the major disadvantages is their low load-bearing capacity under compression and tensile stresses compared to conventional reinforced concrete. Therefore, the functional use of PSPs should be limited to structural elements with minor loading conditions, such as exterior cladding, partitions, and roofing slabs [3]. This also calls for more studies to optimize the effective parameters on the compressive and flexural behaviors of PSPs. Despite the rich literature available about this issue, the number of investigated variables is huge, which makes the analysis of the available experimental data a necessary task.

According to most of the available literature on concrete PSPs, there are several parameters that may influence the mechanical behavior of these panels. Considering only the flexural behavior, which is the focus of this study, it can be said that every parameter influencing the individual strength of concrete layers, the individual and system moments of inertia, and the degree of connection between the two concrete layers would be effective on the flexural behavior, including cracking and ultimate loads, their corresponding deflections, stiffness, and ductility. The reviewed literature showed that the thickness of the concrete layers [4-8], their compressive strength [4, 9-11], the material, distribution, and quantity of their reinforcement [1, 7, 12-15], the geometry and span of the panels [16-18], the type, material, length, configuration, distribution, and quantity of the shear connectors [8, 19-22] are essential parameters that may have significant impact on the flexural response of PSPs. Other parameters, including the type and thickness of the insulation material [23-25] may also have an effect on the deflection and ductility of tested PSP specimens owing to their effect on the panel's moment of inertia.

This study aims to analyze the influence of each of the above parameters on the flexural response of light-weight roofing PSPs that use steel wires as the main flexural reinforcement. The study tries to firstly evaluate the individual effect of each of the influencing parameters, and secondly to introduce statistical models that relate all effective parameters in simple formulas. It is believed that introducing such models, depending on trusted experimental studies, is useful for researchers, where significant literature data are summarized and analyzed, and also useful in practical design, optimization, and implementation of light, low-cost roofing precast concrete sandwich panels, where the statistical models can be used as useful simplified primary pre-design tools to evaluate the initial limits of geometry and reinforcement details.

## 2. Stepwise Regression and Experimental Data

Stepwise regression is a multi-step tool that introduces multivariable regression models based on the analysis of variance that evaluates the probable impact of each variable on the model. Thus, this tool can be considered both a pre-analysis and an analysis tool. The impact of each variable is evaluated statistically using three basic measurements, which are P-value, T-value, and F-value, that decide which of the variables would be carried to the next steps and which variable would be removed based on their significance. The statistical parameters P-, F-, and T-value are measurement tools of different statistical tests and methods to evaluate the effect of a study variable on the behavior of a data set. The statistical null hypothesis assumes that there are no differences between the means of the different groups of samples, which reflects an insignificant effect of the investigated parameters. Decreasing the probability P-value reflects a departure trend from the means, where P-values less than 5% reflects that the null hypothesis is untrue. In ANOVA, the variances of the different data groups are evaluated using the F-value, which also measures the significance of any studied variable. On the other hand, the t-value is a direct result of the t-test that measures the mean departure of a small group of data from a bigger or another group of data, which also evaluates the effectiveness degree of an investigated variable.

The fit of the model is evaluated using the coefficient of determination and its derivatives. In Minitab Statistical Software, three procedures can be used to reach the best model, which are the standard stepwise, forward addition, and backward elimination. The first procedure starts without any variable and conducts simultaneous addition and elimination actions in each step, depending on their P-value, while forward selection starts with zero variables and adds the strongest effect variable in each step based on its statistical parameters. On the other hand, the backwards elimination starts with all variables and eliminates the weakest variable that has the lowest effect on the model and the highest P-value. All procedures stop when all selected variables have P-values less than the specified target. In this study, backwards elimination stepwise regressions were conducted with two-sided intervals of 95% confidence level. This would assure including only effective parameters with a P-value not exceeding 5%.

After a wide survey in the literature, experimental records with inputs (experimental effective parameters) and outputs (results of loads and deflections) were collected in an extended Excel sheet. Due to the lag of essential data, many references were excluded, and an initial set of data of 100 PSP test specimens was included from 15 references [1-15]. Because the current study focuses on light PSPs reinforced with steel wire meshes, the initial set was further filtered by excluding 50 data sets so that the final sheet that is prepared for statistical analysis and stepwise regression includes 50 rows of data. Each row includes 17 columns; 13 of which are input data, while the rest four are the cracking and ultimate loads ($P_{cr}$ and $P_u$) in addition to their corresponding deflections ($\Delta_{cr}$ and $\Delta_u$).

The included parameters that reflect the effect of plate geometry are the plate thickness (L), plate width (W), shear span ($L_s$), thickness of top layer ($T_w$), and thickness of the bottom layer ($B_w$), in addition to the thickness of the insulation core ($I_t$). On the other hand, the parameters related to the connection between the top and bottom layers are the sectional area of the shear connector ($K_A$), the embedment length of the shear connector ($K_L$), the yield strength of the shear connector material ($Kf_y$), and the orientation angle of the shear connector with respect to the horizontal axis of the panel ($K_\alpha$). Finally, the reinforcement ratio ($\rho$) and the yield strength of the main flexural reinforcement ($Rf_y$) are the included parameters of the steel flexural reinforcement. Table 1 below lists the limits of all included input variables in addition to the limits of the associated recorded loads $P_{cr}$ and $P_u$.

Table 1. Limits of experimental records of investigated input and output parameters

| **Parameter** | **$P_{cr}$ (kN)** | **$P_u$ (kN)** | **$F_c$ (MPa)** | **$Rf_y$ (MPa)** | **$\rho$** |
|---|---|---|---|---|---|
| Lower Limit | 3.2 | 8 | 15 | 485 | 0.00167 |
| Upper Limit | 34.3 | 99.3 | 57.7 | 651 | 0.01344 |
| **Parameter** | **L (mm)** | **W (mm)** | **$T_W$ (mm)** | **$B_W$ (mm)** | **$L_S$ (mm)** |
| Lower Limit | 1100 | 400 | 25 | 20 | 200 |
| Upper Limit | 4200 | 1220 | 70 | 75 | 2100 |
| **Parameter** | **$I_t$ (mm)** | **$K_L$ (mm)** | **$K_A$ ($mm^2$)** | **$K_\alpha$ (degree)** | **$Kf_y$ (MPa)** |
| Lower Limit | 20 | 8 | 21.3 | 45 | 400 |
| Upper Limit | 175 | 100 | 314 | 90 | 1012 |

## 3. Analysis of Effective Variables

One of the typical simplified procedures to evaluate the effect of an independent variable on a target dependent variable is to study the direct sole relation between them using a simple relationship. The linear relation is the simplest function that can connect two individual variables, which was therefore selected to conduct basic evaluations for the effects of the 13 independent variables on both cracking load ($P_{cr}$) and ultimate load ($P_u$). Direct linear correlations for $P_{cr}$ and $P_u$ with all included independent variables are summarized in Table 2 and shown in Figures 1 through 13.

As shown in Figure 1, the compressive strength linear correlation with $P_{cr}$ is not good, where $R^2$ is less than 30%, while its correlation with $P_u$ is better, with $R^2$ that is slightly higher than 50%. Despite the fact that these correlations are weak, they actually reflect the strong effect of $F_c$ on both $P_{cr}$ and $P_u$, when the simplification of using linear correlation is taken into account. Moreover, when the correlation of $F_c$ is compared with the other variables shown in Figures 2 to 13, it is clear that the strongest linear relations among all variables are those of $F_c$, where the coefficient of correlation of all other variables for both loads is less than that of $F_c$. Figure 2 clearly shows the minimal direct effect of span length (L) on cracking and ultimate loads, where the correlation line is semi-flat, and the $R^2$ is no more than 4%. A similar behavior is also noticed for the shear span ($L_s$) in Figure 4, insulation thickness ($I_t$) in Figure 7, length of embedment of shear connector ($K_L$) in Figure 8, angle of shear connector ($K_\alpha$) in Figure 10, and reinforcement ratio ($\rho$) in Figure 13. Table 1 shows that the determination coefficients $R^2$ of these parameters are noticeably low, with a maximum value of approximately 6% and a minimum value of as low as 0.13%. On the other hand, Figures 5 and 6 show much better direct linear correlations of the thicknesses of the top and bottom concrete layers ($T_w$ and $B_w$) with the cracking and ultimate loads compared to the above-mentioned variables. The determination coefficients $R^2$ of $T_w$ and $B_w$ reach 44 and 45% as listed in Table 2, which are not individually high values, but reflect the stronger effect of $T_w$ and $B_w$, in addition to $F_c$, on $P_{cr}$ and $P_u$ compared to other investigated variables.

The specimen width (W) and the cross-sectional area of shear connector ($K_A$) showed weaker correlations with $P_{cr}$ and $P_u$ compared to $F_c$, $T_w$ and $B_w$ as shown in Figure 3 and Figure 9 with $R^2$ ranging from approximately 15 to 20% and 10 to 11%, but it is better than the correlations of yield strengths of main steel and shear connector shown in Figures 11 and 12. Thus, it can be summarized that from the direct linear correlations of the investigated parameters with $P_{cr}$ and $P_u$, it can be concluded that $F_c$, $T_w$, and $B_w$ followed by W and $K_A$ seem to have a stronger influence on the flexural cracking and failure loads compared to the other variables. However, it should be mentioned that the individual effect cannot always be considered as an indicator of the in-group effect of an individual independent variable, where group correlations take different paths in some cases, which induces the need to use probability-based analysis of variance instead of depending solely on direct linear correlations.

Table 2. Summary of linear correlations of $P_{cr}$ and $P_u$ with the investigated variables

| **Independent Variable** | **Cracking Load ($P_{cr}$)** | | **Ultimate Load ($P_u$)** | |
|---|---|---|---|---|
| | **Formula** | **$R^2$ (%)** | **Formula** | **$R^2$ (%)** |
| $F_c$ (MPa) | $y = 0.34x + 2.72$ | 29.1 | $y = 1.2x - 7.48$ | 52 |
| L (mm) | $y = 0.0015x + 10.11$ | 3.2 | $y = 0.0044x + 21.09$ | 4.0 |
| W (mm) | $y = 0.011x + 4.84$ | 15.4 | $y = 0.033x + 4.55$ | 20.2 |
| $L_s$ (mm) | $y = 0.0007x + 13.2$ | 0.16 | $y = 0.02x + 30.52$ | 0.13 |
| $T_w$ (mm) | $y = 0.302x + 2.55$ | 20.6 | $y = 1.17x - 11.66$ | 43.7 |
| $B_w$ (mm) | $y = 0.196x + 7.09$ | 11.5 | $y = 1.13x - 6.69$ | 53.6 |
| $I_t$ (mm) | $y = -0.005x + 15.22$ | 6.16 | $y = -007x + 33.97$ | 1.73 |
| $K_L$ (mm) | $y = 0.05x + 12.06$ | 3.65 | $y = 0.078x + 29.28$ | 1.23 |
| $K_A$ ($mm^2$) | $y = 0.037x + 9.28$ | 11.01 | $y = 0.096x + 20.28$ | 10.4 |
| $K_\alpha$ (Degree) | $y = -0.03x + 15.46$ | 0.46 | $y = -0.113x + 38.26$ | 0.92 |
| $Kf_y$ (MPa) | $y = 0.0087x + 8.44$ | 2.73 | $y = 0.037x + 9.29$ | 6.9 |
| $Rf_y$ (MPa) | $y = 0.018x + 4.13$ | 1.25 | $y = 0.029x + 16.17$ | 0.47 |
| ρ | $y = -294.6x + 15.62$ | 1.4 | $y = -196.3x + 33.17$ | 0.9 |

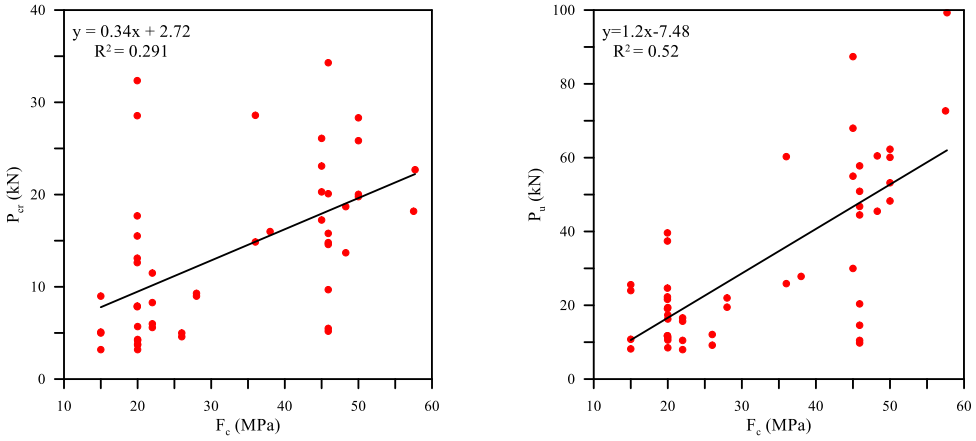


(a) Pcr (b) Pu

**Figure 1** Linear correlation of load with concrete compressive strength (Fc) for (a) $P_{cr}$ and (b) $P_u$

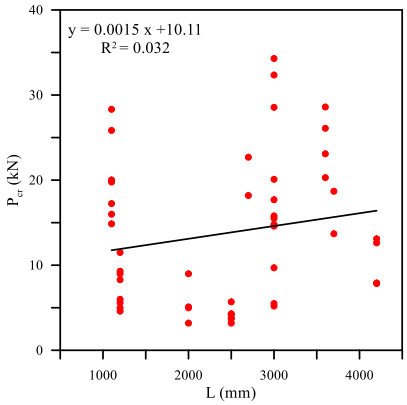


(a) Pcr

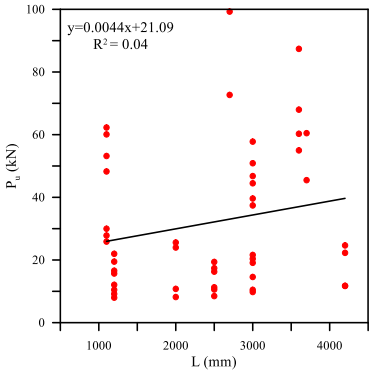


(b) Pu

Figure 2. Linear correlation of load with span length (L) for (a) $P_{cr}$ and (b) $P_u$

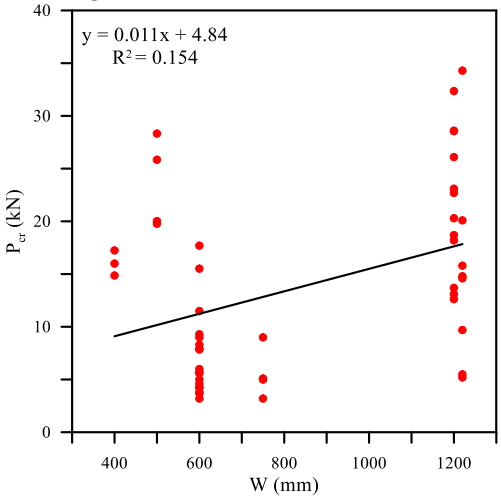


(a) Pcr

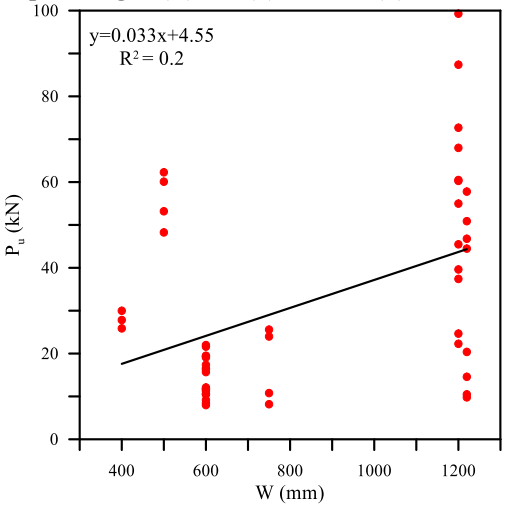


(b) Pu

Figure 3. Linear correlation of load with section width (W) for ((a) $P_{cr}$ and (b) $P_u$

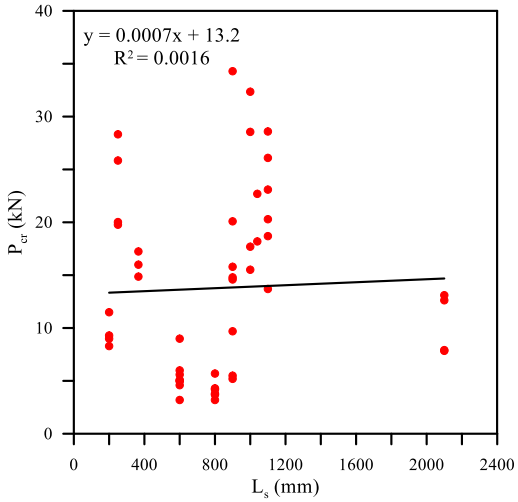


(a) Pcr

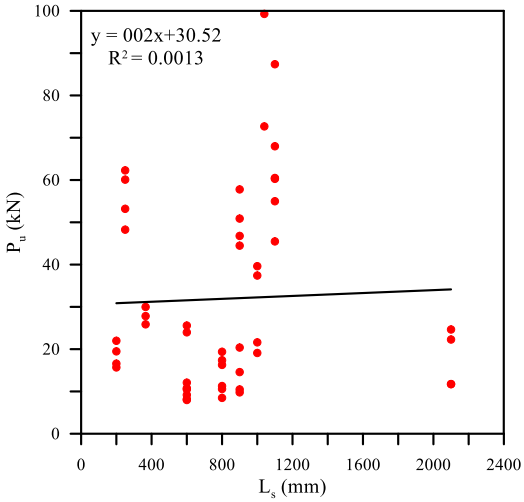


(b) Pu

Figure 4. Linear correlation of load with shear span ($L_s$) for (a) $P_{cr}$ and (b) $P_u$

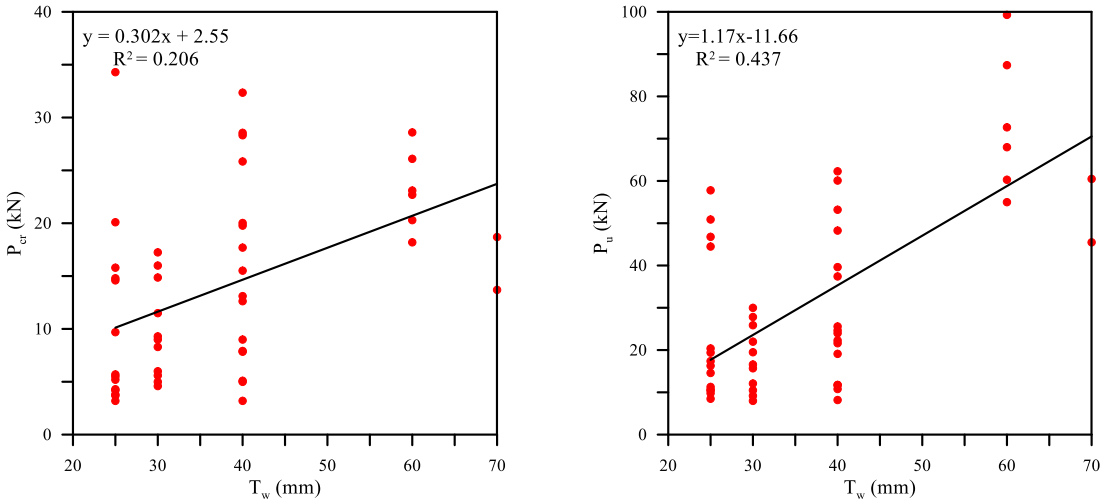


(a) Pcr (b) Pu

Figure 5. Linear correlation of load with top wythe thickness ($T_w$) for (a) $P_{cr}$ and (b) $P_u$

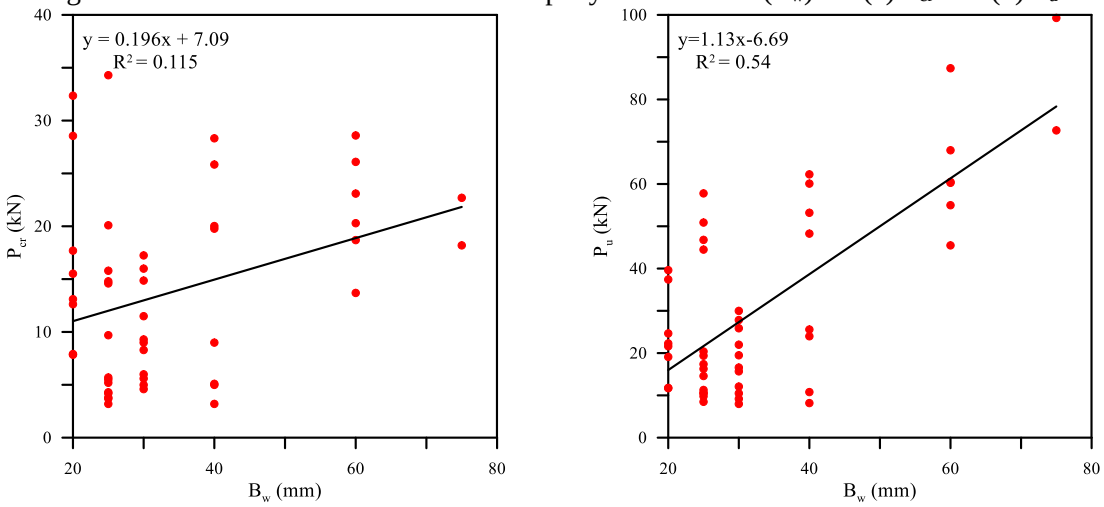


(a) Pcr (b) Pu

Figure 6. Linear correlation of load with bottom wythe thickness ($B_w$) for (a) $P_{cr}$ and (b) $P_u$

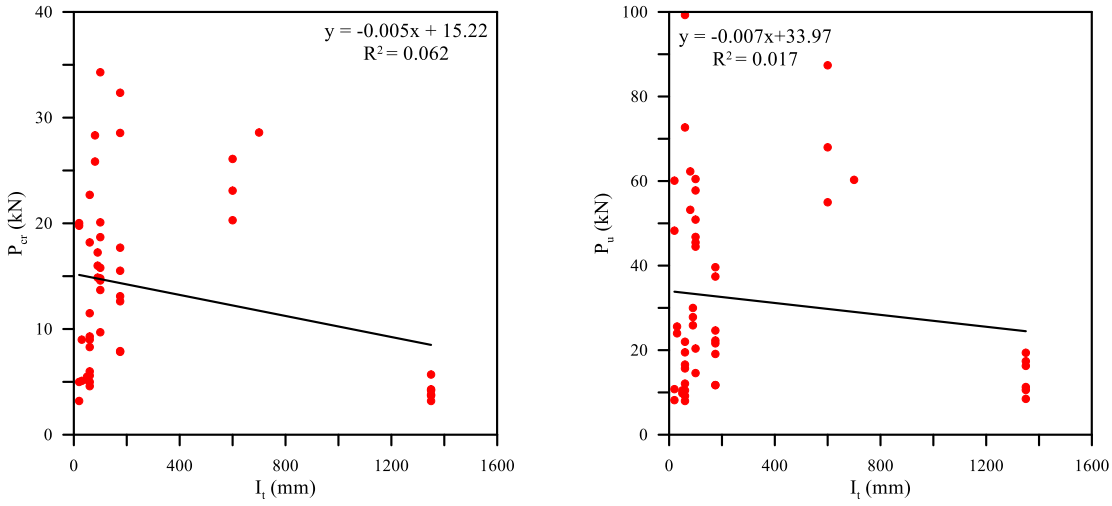


(a) Pcr (b) Pu

Figure 7. Linear correlation of load with insulation thickness ($I_t$) for (a) $P_{cr}$ and (b) $P_u$

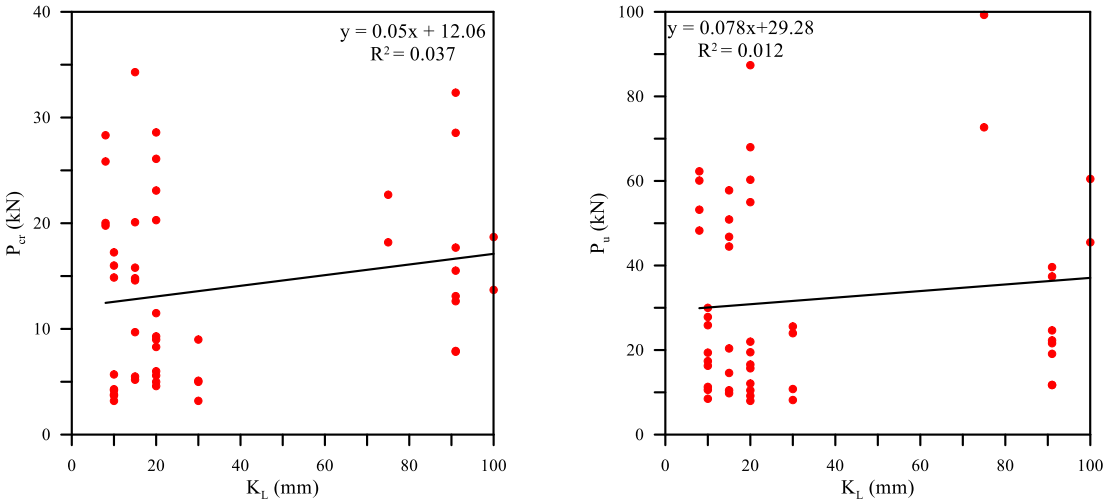


(a) Pcr (b) Pu

Figure 8. Linear correlation of load with shear connector embedment length ($K_L$) for (a) $P_{cr}$ and (b) $P_u$

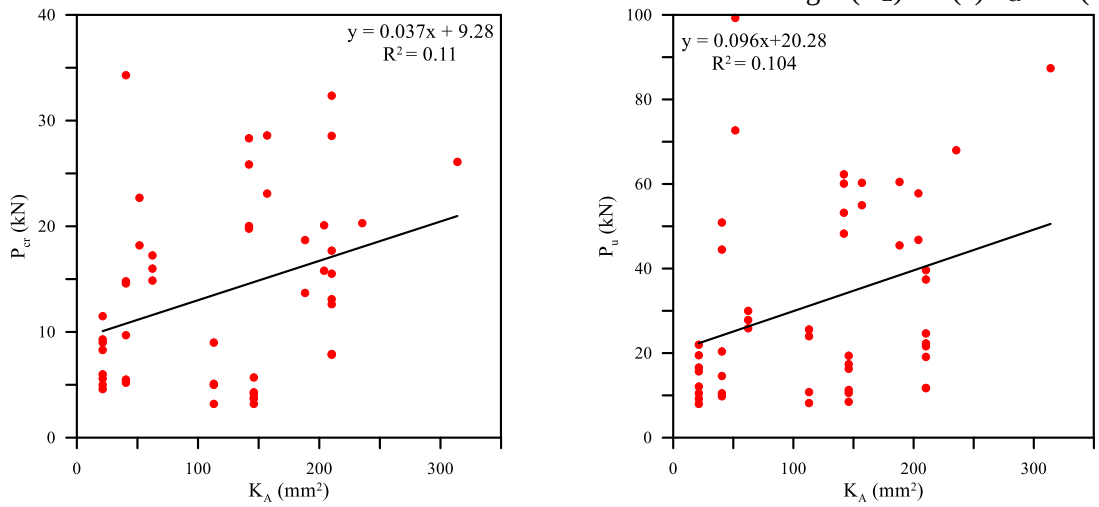


(a) Pcr (b) Pu

Figure 9. Linear correlation of load with shear connector sectional area ($K_A$) (a) $P_{cr}$ and (b) $P_u$

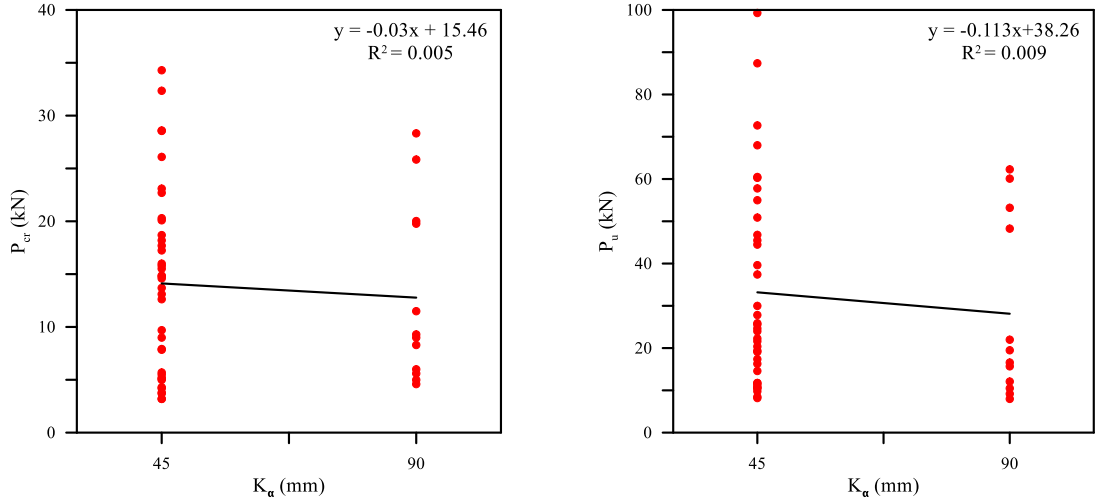


(a) Pcr (b) Pu

Figure 10. Linear correlation of load with shear connector angle ($K_\alpha$) for (a) $P_{cr}$ and (b) $P_u$

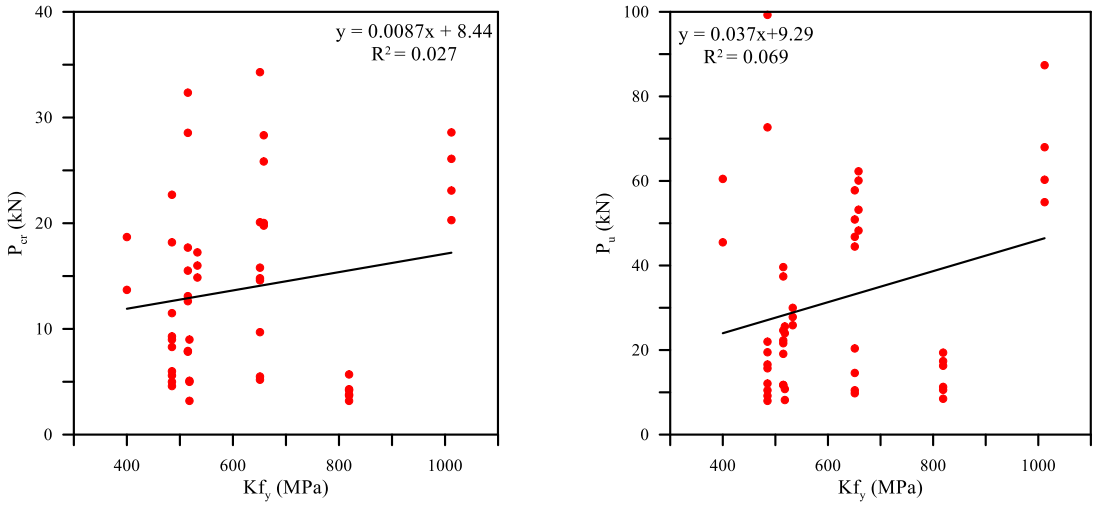


(a) Pcr (b) Pu

Figure 11. Linear correlation of load with shear connector yield strength ($Kf_y$) for (a) $P_{cr}$ and (b) $P_u$

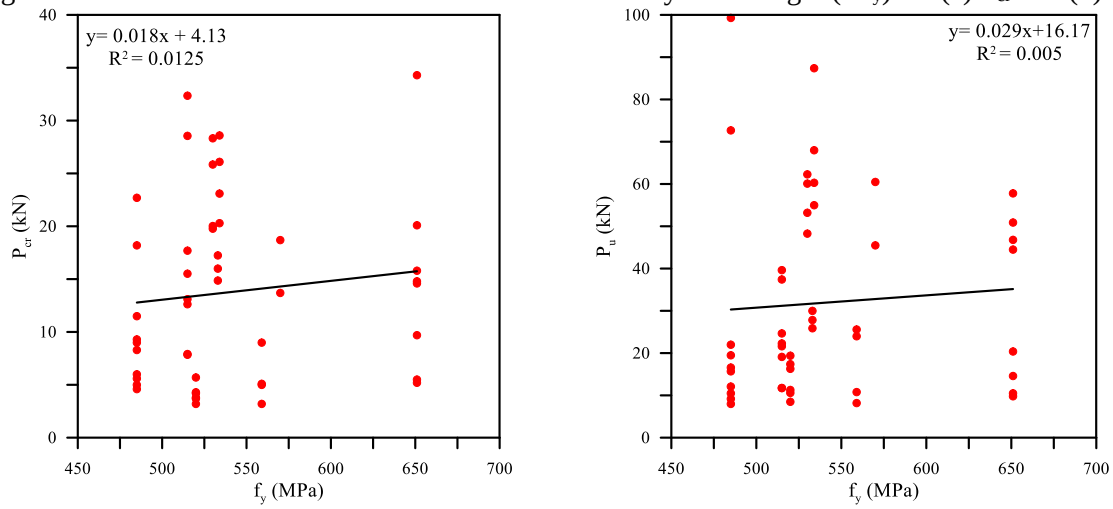


(a) Pcr (b) Pu

Figure 12. Linear correlation of load with reinforcement yield strength ($f_y$) for (a) $P_{cr}$ and (b) $P_u$

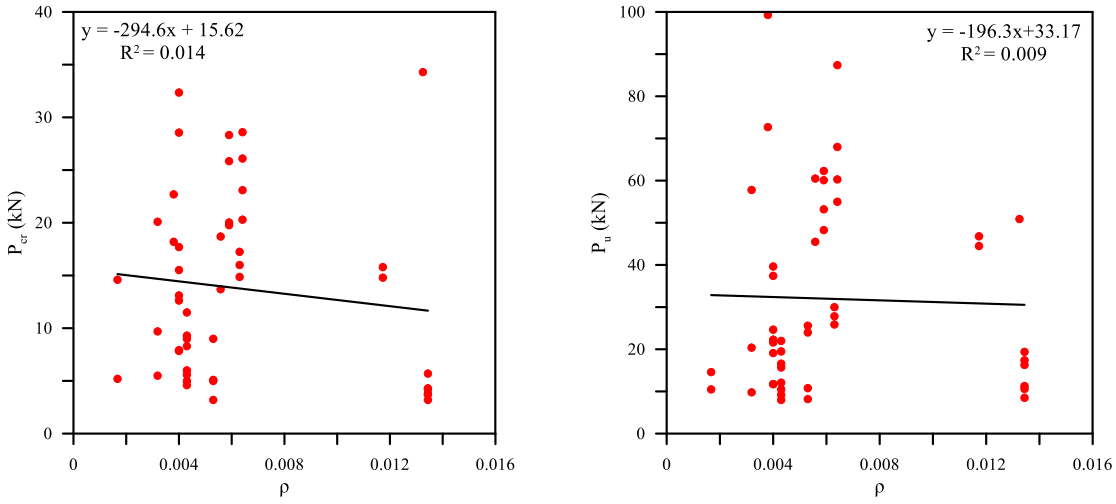


(a) Pcr (b) Pu

Figure 13. Linear correlation of load with reinforcement ratio (ρ) for (a) $P_{cr}$ and (b) $P_u$

## 4. Regression Models

### 4.1 Stepwise regression of $P_{cr}$:

As clarified in the previous section, stepwise regression evaluates the weighted effect of each parameter based on the analysis of variance and probability using three statistical parameters: F-value, T-value, and P-value. Increasing F- and T-values indicate stronger weight in the regression formula, while P-values higher than 0.05 (5%) indicate trivial effects.

The result of the backwards elimination stepwise regression of the cracking load ($P_{cr}$) with the 13 investigated parameters is the formula shown in Table 3, which shows a good fit with $R^2$ of 89.3%. This stepwise regression formula included 10 variables and excluded 3 variables based on their in-group effect on the dependent variable $P_{cr}$. As shown in Table 4, the P-value of the 10 included parameters is less than 0.05, which explains the inclusion of these parameters in the final regression formula. On the other hand, the F- and T-values clarify the weighted effects of each of the 10 parameters, which do not always agree with the preliminary results of the direct linear correlations. It is obvious in the table that the highest F- and T-values were recorded for $f_y$, L, and $F_c$, which reflects their stronger effect on the regression formula compared to the rest of the parameters, where their F-value exceeded 50, and their minimum T-value was approximately 8. The second effective group of variables was W, $T_w$, $I_t$, with a minimum F-value and T-value of approximately 20 and 4, respectively. Figure 14(a) shows the normal probability plot of the regression equation, which clearly reflects a good fit with small residuals not exceeding 2.5 kN as shown in Figure 14(b), where all experimental records fall around and close to the red reference line.

Table 3. Step-wise regression summary of $P_{cr}$

| | |
|---|---|
| **Regression Equation** | $P_{cr} = 10.55 + 0.38\ Fc - 0.011\ L + 0.015\ W + 0.546\ T_W - 0.34\ B_W + 0.098\ I_t + 0.04\ K_A - 0.132\ K_\alpha - 0.0216\ f_y + 476\ \rho$ |
| **$R^2$ (%)** | 89.28 |
| **Included Variables** | $Fc$ , $L$ , $W$ , $T_W$ , $B_W$ , $I_t$ , $K_A$ , $K_\alpha$ , $f_y$ , $\rho$ |
| **Excluded Variables** | $L_s$ , $K_L$ , $Kf_y$ |

Table 4. Analysis of variance and step-wise regression details of $P_{cr}$

| Variable | F-Value | T-Value | P-Value | Coefficient |
|---|---|---|---|---|
| $F_c$ (MPa) | 63.23 | 7.95 | 0.000 | 0.3796 |
| L (mm) | 78.02 | -8.83 | 0.000 | -0.01112 |
| W (mm) | 32.83 | 5.73 | 0.000 | 0.01495 |
| $T_w$ (mm) | 21.34 | 4.62 | 0.000 | 0.546 |
| $B_w$ (mm) | 10.64 | -3.26 | 0.002 | -0.339 |
| $I_t$ (mm) | 40.95 | 6.40 | 0.000 | 0.0980 |
| $K_A$ ($mm^2$) | 19.37 | 4.40 | 0.000 | 0.0396 |
| $K_\alpha$ (Degree) | 14.62 | -3.82 | 0.000 | -0.1324 |
| $f_y$ (MPa) | 95.35 | -9.76 | 0.000 | -0.02155 |
| $\rho$ | 5.45 | 2.33 | 0.025 | 476 |

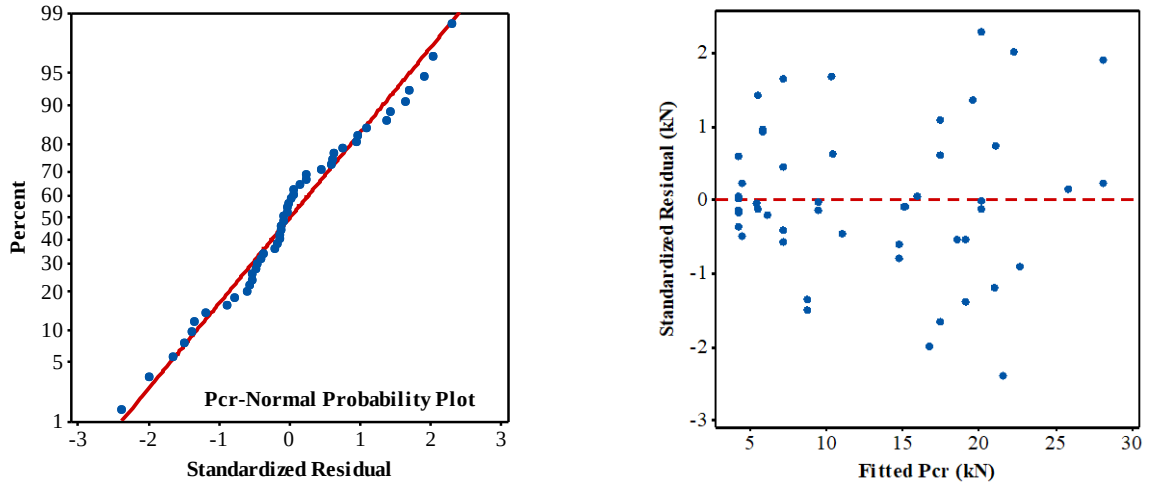


(a) Normal probability plot (b) Residuals-fit

Figure 14. Stepwise regression plots of $P_{cr}$ (a) normal probability (b) Residuals vs. fit

**4.2 Stepwise regression of $P_u$:**

The summary of the stepwise regression of the ultimate load is given in Table 4. As listed in the table, a very good fit was obtained with a high coefficient of determination $R^2$ of 92.6%. The obtained formula includes 8 out of the 13 parameters, as shown in Table 5. All P-values of the included parameters are significantly lower than 5%, as listed in Table 6, which reflects their in-group high impact on the fit of $P_u$. It is also obvious in the table that the compressive strength of the mixture has the highest effect among the eight included parameters, with F- and T-values of approximately 62 and 7.9, respectively, followed by the thickness of the bottom wythe (layer) and the cross-sectional area of the shear connector with F- and T-values of approximately 53 and 7.3, and 45 and 6.7, respectively. However, the rest parameters also showed significant F- and T-values as shown in Table 6, reflecting significant influence on the fit. The strength of the fit is illustrated in Figure 15, where the residuals in Pu are limited to a maximum value of approximately 3 kN.

Table 5. Stepwise regression summary of $P_u$

| | |
|---|---|
| **Regression Equation** | Pu = -35.26 + 0.84 Fc - 0.013 L + 0.0234 W + 0.94 $B_W$ + 0.21 $I_t$ + 0.13 $K_A$ - 0.04 $f_y$ + 2094 ρ |
| **$R^2$ (%)** | 92.62 |
| **Included Variables** | Fc , L , W , $B_W$ , $I_t$ , $K_A$ , $f_y$ , ρ |
| **Excluded Variables** | $L_s$ , $T_W$ , $K_L$ , $K_α$ , $Kf_y$ |

Table 6. Analysis of variance and step-wise regression details of $P_u$

| Variable | F-Value | T-Value | P-Value | Coefficient |
|---|---|---|---|---|
| $F_c$ (MPa) | 62.03 | 7.88 | 0.000 | 0.844 |
| L (mm) | 29.00 | -5.39 | 0.000 | -0.01282 |
| W (mm) | 15.79 | 3.97 | 0.000 | 0.02339 |
| $B_w$ (mm) | 52.94 | 7.28 | 0.000 | 0.936 |
| $I_t$ (mm) | 25.03 | 5.00 | 0.000 | 0.2097 |
| $K_A$ ($mm^2$) | 45.12 | 6.72 | 0.000 | 0.1302 |
| $f_y$ (MPa) | 31.36 | -5.60 | 0.000 | -0.03974 |
| ρ | 17.43 | 4.18 | 0.000 | 2094 |

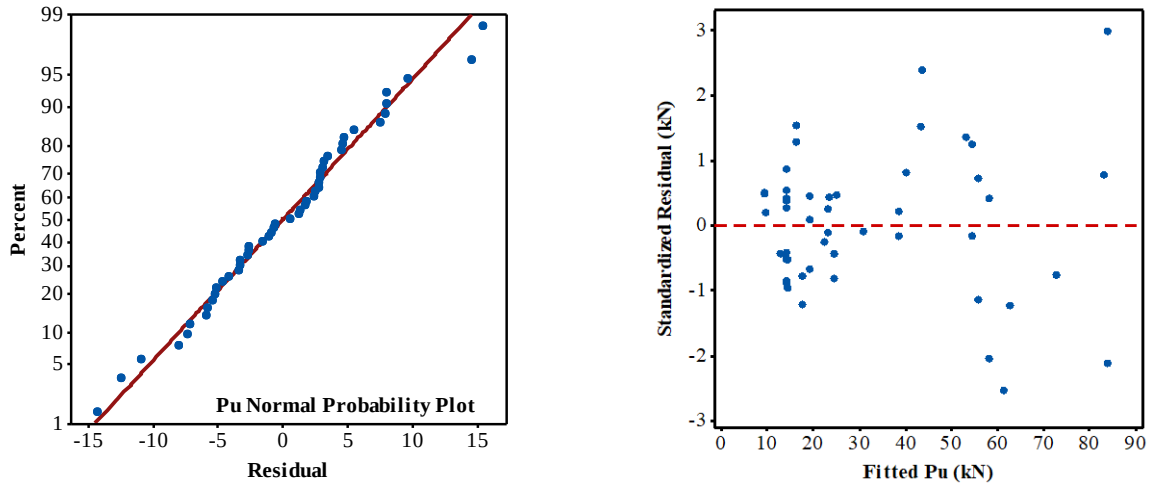


(a) Normal probability plot (b) Residuals-fit

Figure 15. Stepwise egression plots of $P_u$ (a) normal probability (b) Residuals vs. fit

## 5. Conclusions

This study attempted to analyze the effective parameters on the flexural behavior of precast concrete sandwich panels. Parameters related to the geometry, strength, and material properties of the panel and its outer concrete layers, inner insulation core, and shear connectors were investigated. The main concluding remarks from the current study can be summarized in the followings:

1- Direct individual correlations for each of the 13 investigated parameters with cracking load ($P_{cr}$) and ultimate load ($P_u$) showed that none of these parameters has a dominant role on the retained load capacities, where the correlations retained $R^2$ values ranged from less than 1% to 53.6%, which means that none of the investigated parameters can solely represent the load capacity with adequate level of confidence.

2- The direct correlations showed that the compressive strength and thickness of the concrete layers have the best fits with the ultimate load capacity compared to the other investigated parameters, with $R^2$ values ranging from 43.7 to 53.6%.

3- The final outputs of the backwards stepwise regressions of $P_{cr}$ and $P_u$ included variables that showed P-values less than 5%, which are most of the investigated parameters, while parameters like $L_s$, $K_L$, $Kf_y$ were eliminated due to their trivial impact on the regression formulas represented by their high P-values.

4- The T- and F-values of the compressive strength of concrete and the thickness of the bottom layer were among the highest values, confirming the direct correlation results of their higher impacts compared to the other parameters. However, parameters like span length, sectional area of shear connectors, and yield strength of flexural reinforcement also showed high T- and F-values, revealing a significant impact on the stepwise regressions.

5- The obtained stepwise regression model of the flexural capacity represented by the ultimate load strength can be considered a reliable simplified pre-analysis tool that can be used with an adequate degree of confidence, where the $R^2$ of the formula exceeds 92%.

## Declaration of Competing Interest

The authors declare that there are no conflicts of interest regarding the publication of this manuscript.

## Funding Information

No funding was received from any financial organization to conduct this research

## Author Contributions

Khaldoon S. A. Altameemi conducted the literature review, collected the analysis data, and partially collaborated on writing the original article draft. Omar M. H. Chlaibawi conducted the statistical analysis and data verification together with Sallal R. Abid, who is also collaborating on writing the original draft of the article. Sallal R. Abid and Mustafa Özakça finalized the article visualization and reviewed/edited the final article draft. All the authors discussed the results and the final version of this article.

## Acknowledgments

The authors express their gratitude to Wasit University/ College of Engineering/Civil Engineering department in Kut, Wasit, Iraq, for supporting this study.

**References**

[1] N. Guerrero, J. Carrillo, R. I Herrera, M. E. Marante, "Experimental and numerical investigation on the behavior of concrete sandwich", *Journal of Building Engineering*, vol. 86, 108930, 2024.
[2] S. M. Bida, F. N. A. Abdul Aziz, M. S. Jaafar, F. Hejazi, N. AbuBakar," Thermal Resistance of Insulated Precast Concrete Sandwich Panels", *International Journal of Concrete Structures and Materials*, vol. 15, 6216, 2021.
[3] F. Refaie, R. Abbas, F. H. Fouad (2020), "Sustainable construction system with Egyptian metakaolin based geopolymer concrete sandwich panels", *Case Studies in Construction Materials*, vol. 13, e00436, 2020.
[4] A. B. Awan, F. U. A. Shaikh. "Structural behavior of recycled tire crumb rubber sandwich panel in flexural bending. Structural Concrete", vol. 22, PP 3602-3619, 2021.
[5] K. Choi, W. Choi, L. Feo, S. Jang, H. Yun," In-Plane Shear Behavior of Insulated Precast Concrete Sandwich Panels Reinforced with Corrugated GFRP Shear Connectors", *Composites Part B*: *Engineering*, vol. 76, Pages 1-354, 2015.
[6] J. Daniel Ronald Joseph, J. Prabakar a, P. Alagusundaramoorthy, (2017)," Precast concrete sandwich one-way slabs under flexural loading", *Engineering Structures*, vol. 138, PP 447–457, 2017.
[7] J. D. R. Joseph, J. Prabakar, P. Alagusundaramoorthy, "Insulated precast concrete sandwich panels under punching and bending", *PCI Journal (ISSN 0887-9672)*, vol. 64, No. 2, 68-79, March–April 2019.
[8] M. Fahmy, W. Attia, A. A. Al Sayed, H. Ibrahim, "Shear performance of X and Z configuration wythe ties for insulated precast concrete sandwich panels using different FRP materials", *Journal of Building Engineering*, vol 85, 108701, 2024.
[9] M. Zhang; W. Feng, K. Chen, B. Li, "Flexural Behavior of a New Precast Insulation Mortar Sandwich Panel", *Applied Sciences*, vol. 14, 2071, 2024.
[10] I. Choi, J. Kim, H. Kim, "Composite Behavior of Insulated Concrete Sandwich Wall Panels Subjected to Wind Pressure and Suction", *Materials*, vol 8, 1264-1282, 2015.
[11] D. Tomlinson, A. Fam, " Flexural behavior of precast concrete sandwich wall panels with basalt FRP and steel reinforcement", *PCI Journal*, vol 60, (6):51-71, 2015.
[12] J, Kim, Y. You," Composite Behavior of a Novel Insulated Concrete Sandwich Wall Panel Reinforced with GFRP Shear Grids: Effects of Insulation Types", *Materials*, vol 8, 899-913, 2015.
[13] K. Hodicky, T. Hulin, J.W. Schmidt, H. Stang, "Structural performance of new Thin-Walled Concrete Sandwich Panel System Reinforced with BFRP Shear Connecters", *Fourth Asia-Pacific Conference on FRP in Structures© 2013 International Institute for FRP in Construction*, 11-13, December 2013.
[14] M. Flansbjer, N. W. Portal, D. Vennetti, U. Mueller, (2018)," Composite Behaviour of Textile Reinforced Reactive Powder Concrete Sandwich Façade Elements", *Flansbjer et al. Int J Concr Struct Mater*, vol. 12, 71, 2018.
[15] Elvira. (2024). "Utilizing Fiber Mesh and Nylon Rope as Non-Steel Reinforcement for Sandwich Concrete Plate Precast in Coastal Area Structures". *Jurnal Teknik Sipil (JTS*), vol. 24, 2. p.964-978, 2025.
[16] Y. Li, S. Yin, and L. Feng, "Test and analysis of the flexural performance of sandwich insulation wall panels with textile-reinforced engineered cementitious composites in wythes after hot rain cycles", *Journal of Industrial Textiles*, vol. 54, pp 1–28, 2024.
[17] U. Skadiņš, K. Kuļevskis, A. Vulāns, R. Brencis. "Thin-Layer Fibre-Reinforced Concrete Sandwich Walls: Numerical Evaluation ". *Journals Fibers*, vol. 11, Issue 2, no. 2: 19, 2023.

[18] K. I. Alev, M. O. Kaman, M. Albayrak, C. Yanen. "Investigation of the mechanical response of laminated composites reinforced with different type wire mesh", *Journal of the Brazilian Society of Mechanical Sciences and Engineering*, vol. 45, 475, 2023
[19] N. Mohamad, A. I. Khalil, A. A. Abdul Samad, W. I. Goh, "Structural Behavior of Precast Lightweight Foam Concrete Sandwich Panel with Double Shear Truss Connectors under Flexural Load", *Hindawi Publishing Corporation ISRN Civil Engineering*, vol. 2014, Article ID 317941, 7 pages, 2014.
[20] S. M. Bida, F. N. A. Abdul Aziz, M. S. Jaafar, F. Hejazi, A. Nabilah, " Advances in Precast Concrete Sandwich Panels toward Energy Efficient Structural Buildings ", *Applied Engineering and Technology*, vol. 3, No. 1, pp. 58-69, April 2024.
[21] H. Kazem, W. G. Bunn, H. M. Seliem, S. H. Rizkalla, H. Gleich. "Durability and long-term behavior of FRP/foam shear transfer mechanism for concrete sandwich panels", *Construction and Building Materials*, vol. 98, 722–734, 2015.
[22] Y. Wang, J. Wang, D. Zhao, G. Hota, R. Liang, D. Hui, "Flexural Behavior of Insulated Concrete Sandwich Panels using FRP-Jacketed Steel-Composite Connectors", *Hindawi, Advances in Materials Science and Engineering*, vol. 2022, Article ID 6160841, 25 pages, 2022.
[23] S. Gopinath, V. R. Kumar, H. Sheth, A. R. Murthy, N. R. Iyer, "Pre-fabricated sandwich panels using cold-formed steel and textile reinforced concrete", *Construction and Building Materials*, vol. 64, 54–59, 2014.
[24] S. Schiavoni, F. D'Alessandro, F. Bianchi, F. Asdrubali, "Insulation materials for the building sector: A review and comparative analysis", *Renewable and Sustainable Energy Reviews*, vol. 62, 988–1011, 2016.
[25] L. Adityaa, T.M.I. Mahliaa, B. Rismanchic, H.M. Nge, M.H. Hasane, H.S.C. Metselaare, Oki Murazaf, H.B. Aditiyab, "A review on insulation materials for energy conservation in buildings", *Renewable and Sustainable Energy Reviews*, vol. 73, 1352–1365, 2017.